However, for two dimensions, integration of Eq. (14) gives

$$L=\int_0^\infty g\,dr=\int_0^\infty d(fr)$$

$$=0$$

Furthermore, for two dimensions, second differentiation of Eq. (14) produces

$$\lambda_g=(1/\sqrt{3})\lambda_f$$

The surprising result that L *always* equals zero in two-dimensional turbulence indicates that the Taylor definition of the averaged size of eddy [Eq. (15)] may not have real significance, certainly for two-dimensional turbulence. Apparently, L_f would be a more significant definition.

Loss of Kinetic Energy of Turbulence

The time rate of loss of turbulent energy per unit volume for two dimensions is:

$$-\frac{1}{2}\rho\frac{d}{dt}(\overline{u^2}+\overline{v^2})=-\rho\frac{\overline{du^2}}{dt}=\frac{8}{3}\mu\overline{\left(\frac{\partial u}{\partial v}\right)^2} \tag{16}$$

Now, generally, according to Taylor,

$$\frac{\overline{u^2}}{\lambda_g{}^2}=\frac{1}{2}\overline{\left(\frac{\partial u}{\partial y}\right)^2}$$

Hence, from Eq. (16),

$$\frac{\overline{du^2}}{dt}=-\frac{16}{3}\nu\frac{\overline{u^2}}{\lambda_g{}^2}$$

in two dimensions compared to

$$\frac{\overline{du^2}}{dt}=-10\nu\frac{\overline{u^2}}{\lambda_g{}^2}$$

in three dimensions.

References

[1] Taylor, G. I., "Statistical Theory of Turbulence," *Proceedings of the Royal Society*, A151, 1935, pp. 421-478.

[2] von Kármán, T. and Howarth, L., "On the Statistical Theory of Isotropic Turbulence," *Proceedings of the Royal Society*, A164, 1938, pp. 192-215.

Finite-Element Stress Analysis of Axisymmetric Bodies under Torsion

Tien-Yu Tsui*

Army Materials and Mechanics Research Center
Watertown, Mass.

Introduction

THE present study is motivated by the consideration of the stress analysis of artillery projectiles. During firing, the projectile is subjected to a combination of various loads which are: 1) axial load, due to linear acceleration of the projectile; 2) centrifugal load, due to angular rotation of the projectile; 3) torsional load, due to angular acceleration of the projectile; 4) internal load due to setback on H.E.; and 5) external load, due to gun tube constraint, band pressure, and balloting. In view of the complexity of the geometry of the projectile, a finite-element analysis must be performed in order to determine the stresses and deformations in the projectile. Since the projectile has an axis of rotational symmetry, it is only logical that an axisymmetric ring element would model it more accurately and efficiently. In an MIT study,[1] which was performed for AMMRC under contract, an axisymmetric ring element was developed based on the assumed-stress hybrid finite-element model. However, it can only treat axisymmetric loads of the projectile.

It is the goal of the present analysis to develop an axisymmetric solid-of-revolution element which can be used to determine the stresses and deformations in axisymmetric structural bodies under torsional loads. The assumed-stress hybrid model is employed to derive the element stiffness matrix such that the results can be combined with those from the MIT study.

Other finite-element formulations for solution of axisymmetric structural bodies under torsion can also be made. The axisymmetric quadrilateral element, based on the displacement formulation in the ANSYS finite-element program,[2] can be used for modeling axisymmetric structures with nonaxisymmetric loadings, such as bending, shear, or torsion. Different finite-element formulations have also been developed for the solution of torsion of nonprismatic bars.[3,4]

Formulation

The formulation of the element stiffness matrix is based on the assumed-hybrid model.[5] Since only structural problems in the shape of body of revolution are considered, an axisymmetric solid-of-revolution ring element is developed. The ring element has four modes and a general quadrilateral cross section. For convenience, the field equations in the cylindrical coordinates are used with u, v, and w denote, respectively, the components of displacement in the radial r, tangential θ, and axial z directions. In the solution of torsional problems, the semi-inverse method may be used and the components of displacement u and w are assumed to be zero. It can be shown that the solution obtained on the basis of such an assumption satisfies all the equations of elasticity and, therefore, represents the true solution of the problem.[6] Substituting $u=w=0$ in the six strain-displacement relationships and, making use of the fact that from symmetry the displacement v does not vary with the angle θ, one obtains:

$$\epsilon_r=\epsilon_\theta=\epsilon_z=\gamma_{rz}=0$$

$$\gamma_{r\theta}=\frac{\partial v}{\partial r}-\frac{v}{r},\quad \gamma_{\theta z}=\frac{\partial v}{\partial z} \tag{1}$$

From Eq. (1) and Hooke's law, it can be seen that of all the six stress components, only $\tau_{r\theta}$ and $\tau_{\theta z}$ are different from zero. As a result of this and the symmetry condition, two of the equilibrium equations are identically satisfied and the third one becomes:

$$\frac{\partial\tau_{r\theta}}{\partial r}+\frac{\partial\tau_{\theta z}}{\partial z}+\frac{2\tau_{r\theta}}{r}=0 \tag{2}$$

Hence, in the subsequent formulation of an axisymmetric solid-of-revolution ring element, one is only concerned with the displacement v and the equilibrium equation given by Eq. (2).

The assumed-stress hybrid model is based on a modified complementary energy principle. It assumes compatible displacements along the interelement boundaries and a stress

Received Sept. 28, 1977; revision received Aug. 2, 1978. This paper is declared a work of the U.S. Government and therefore is in the public domain.

Index category: Structural Statics.

*Mechanical Engineer, Mechanics Research Laboratory.

Table 1 Comparison of finite-element solution and exact solution (hollow cylinder) (length of cylinder = 12 in., outer radius = 3.0 in., inner radius = 1.5 in., torque = 5000 in.-lb)

Exact solution	Location (z) (r)	96 elements 0.75	96 elements 1.50	96 elements 2.25	24 elements 1.5	24 elements 3.0	24 elements 4.5	8 elements 3.0	8 elements 6.0
62.88	1.50	62.96	62.89	62.87	62.87	62.91	62.85	62.54	63.00
73.36	1.75	73.38	73.37	73.34					
83.83	2.00	83.87	83.84	83.71	83.71	83.89	83.81		
94.31	2.25	94.33	94.31	94.31				93.69	94.57
104.79	2.50	104.77	104.78	104.80	104.60	104.80	104.81		
115.27	2.75	115.19	115.26	115.28					
125.75	3.00	125.55	125.80	125.72	125.27	125.93	125.66	124.85	126.17

Table 2 Comparison of finite-element solution and exact solution (truncated cone) (length of cone = 12 in., small-end radius = 1.5 in., large-end radius = 3.0 in., torque = 5000 in.-lb)

Location z	Location r	$\tau_{z\theta}$ Exact	$\tau_{z\theta}$ 96 elements	$\tau_{z\theta}$ 24 elements	$\tau_{r\theta}$ Exact	$\tau_{r\theta}$ 96 elements	$\tau_{r\theta}$ 24 elements
1.5	1.687	653.73	564.73	930.52	81.69	95.53	24.71
3.0	1.875	476.70	455.14	384.60	59.59	60.76	70.10
4.5	2.062	358.07	353.93	403.34	41.75	43.13	30.71
6.0	2.25	275.87	276.03	263.42	34.48	32.42	33.26
7.5	2.437	216.94	218.00	225.63	27.11	25.25	21.76
9.0	2.625	173.72	174.74	173.97	21.72	20.16	19.57
10.5	2.813	141.27	141.91	139.62	17.66	16.33	13.17

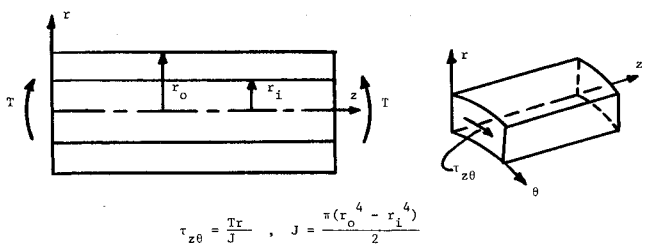

$$\tau_{z\theta} = \frac{Tr}{J}, \quad J = \frac{\pi(r_o^4 - r_i^4)}{2}$$

Fig. 1 Torsion of hollow cylinder.

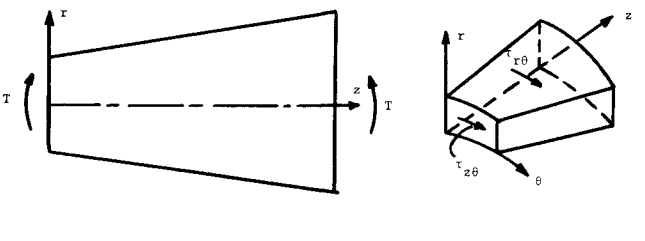

$$\tau_{\theta z} = -\frac{crz}{(r^2+z^2)^{5/2}}, \quad \tau_{r\theta} = -\frac{cr^2}{(r^2+z^2)^{5/2}}$$

$$c = -\frac{T}{2\pi\left(\frac{2}{3} - \cos\alpha + \frac{1}{3}\cos^3\alpha\right)}$$

Fig. 2 Torsion of truncated cone.

field which satisfies equilibrium within each element. In the present study, the same linear interpolation function employed in Ref. 1 is selected to assure the displacement compatibility between neighboring elements. Within each element, the following stress field is chosen to satisfy the equilibrium equation:

$$\tau_{r\theta} = \beta_1 + \beta_2 r + \beta_3 z$$

$$\tau_{\theta z} = \beta_4 + \beta_5 r + \beta_6 z \tag{3}$$

Substituting Eq. (3) into Eq. (2), one obtains

$$\beta_2 + \beta_6 + 2\beta_1/r + 2\beta_2 + 2\beta_3 z/r = 0 \tag{4}$$

In order for the assumed stress to satisfy the equilibrium equation exactly, the following relationships must hold:

$$3\beta_2 + \beta_6 = 0, \quad 2\beta_1 = 0, \quad 2\beta_3 = 0 \tag{5}$$

As a result, the assumed stress becomes

$$\tau_{r\theta} = \beta_2 r, \quad \tau_{z\theta} = \beta_4 + \beta_5 r - 3\beta_2 z \tag{6}$$

After the completion of the selections of the interpolation function and the stress field for the element, one can proceed to calculate the element stiffness matrix. The reader is referred to Ref. 1 for steps in details.

Numerical Example

In order to examine the adequacy of the element developed in this study, it is employed to analyze two problems with known analytical solutions. The first problem is the torsion of a hollow cylinder (Fig. 1) and the second is the torsion of a truncated cone (Fig. 2). The exact solution[6] of each problem is given along with the figure.

The results of the finite-element solution of these problems compared with the exact solutions are shown in Tables 1 and 2. Study of the convergence of the finite-element solutions vs the total number of elements used is also indicated in the tables. As can be seen, an excellent comparison is obtained between the finite-element solutions and the exact solutions in the solid cylinder case for the various mesh sizes employed. In the case of truncated cone, excellent agreement is achieved for the stress in the larger mesh size case.

It should be added here that other forms of stress assumptions were also studied, including second- and third-order terms. However, less than satisfactory results were obtained.

References

[1] Spilker, R. L., "A Study of Elastic-Plastic Analysis by the Assumed-Stress Hybrid Finite Element Model, With Application to

Thick Shells of Revolution," AMMRC CTR 74-71 (also MIT ASRL TR 175-1), Dec. 1974.

[2]DeSalvo, G. J. and Swanson, J. A., "ANSYS, Engineering Analysis System," Swanson Analysis Systems, Inc., March 1, 1975.

[3]Krahula, J. L. and Lauterbach, G. F., "A Finite Element Solution for Saint-Venant Torsion," *AIAA Journal*, Vol. 7, Dec. 1969, pp. 2200-2203.

[4]Herrmann, L. R., "Elastic Torsional Aalysis of Irregular Shapes," *Proceedings of the American Society of Civil Engineers, Journal of the Engineering Mechanics Division*, Vol. 91, No. EM6, Pt. 1, Dec. 1965.

[5]Pian, T.H.H., "Derivation of Element Stiffness Matrix by Assumed Stress Distributions," *AIAA Journal*, Vol. 2, July 1969, pp. 1333-1336.

[6]Timoshenko, S. and Goodier, J. N., *Theory of Elasticity*, 2nd ed., McGraw-Hill, New York, 1951.

Approximate Hemispherical Radiative Properties

D. C. Look*
University of Missouri—Rolla, Rolla, Mo.

Introduction

THE several investigations of radiative properties of surfaces that have appeared in the literature[1-3] have dealt primarily with emissive characteristics and, in particular, with the estimates of the monospectral hemispherical emittance. These estimates depend on the optical constants of the emitting material, that is, the real portion of the index of refraction n_λ, the imaginary portion of the index of refraction, k_λ ($N_\lambda = n_\lambda(1 - ik_\lambda)$), and the receiving material N_0. The subscript λ indicates wavelength dependence. It is usually conceded that the hemispherical properties are more easily estimated when the normal emittance is known or can be determined. This is a convenience which stems from the fact that emittance measurements are often performed at or near normal and charts of the ratio of the hemispherical emittance to the normal emittance are available.[2,3] These charts have been made available after long numerical integrations, but only for a few values of n_λ and k_λ.

Approximate closed-form expressions of the monospectral hemispherical emittance have been obtained under the condition that $n_\lambda^2(1 + k_\lambda^2)$ be very large compared to unity. The resulting approximation is essentially exact in the cases where n_λ and k_λ are greater than unity (typical of metals in the infrared regions). In the case where the refractive index is less than unity, a large error results. Hering[3] has set forth various accuracy criteria for n_λ and k_λ.

The purpose of this Note is to indicate another approximation for monospectral hemispherical emittance determined from the monospectral hemispherical reflectance (i.e., $\epsilon_h(\lambda) = 1 - \rho_h(\lambda)$).

Development

The expressions from electromagnetic theory that represent the monospectral, specular reflectance of nonmagnetic material polarized perpendicular to, $\rho_\perp(\phi,\lambda)$, and parallel to, $\rho_\parallel(\phi,\lambda)$, the plane of incidence can be stated as[4]:

$$\rho_\perp(\phi,\lambda) = \frac{a^2 + b^2 - 2a\cos\phi + \cos^2\phi}{a^2 + b^2 + 2a\cos\phi + \cos^2\phi} \tag{1}$$

$$\rho_\parallel(\phi,\lambda) = \frac{\rho_\perp(\phi,\lambda)\,(a^2 + b^2 - 2a\sin\phi\tan\phi + \sin^2\phi\tan^2\phi)}{(a^2 + b^2 + 2a\sin\phi\tan\phi + \sin^2\phi\tan^2\phi)} \tag{2}$$

where

$$2a^2 = \{[n_\lambda^2(1 - k_\lambda^2) - \sin^2\phi]^2 + 4n_\lambda^4 k_\lambda^2\}^{1/2} + n_\lambda^2(1 - k_\lambda^2) - No^2\sin^2\phi \tag{3}$$

and

$$2b^2 = \{[n_\lambda^2(1 - k_\lambda^2) - \sin^2\phi]^2 + 4n_\lambda^4 k_\lambda^2\}^{1/2} - n_\lambda^2(1 - k_\lambda^2) + No^2\sin^2\phi \tag{4}$$

In these equations, ϕ is the angle of incidence. For the case of natural or equally polarized light, the angular monospectral reflectance is the average of these polarized components:

$$\rho(\phi,\lambda) = \frac{\rho_\perp(\phi,\lambda) + \rho_\parallel(\phi,\lambda)}{2} \tag{5}$$

The monospectral hemispherical reflectance $\rho_h(\lambda)$ as defined by Sparrow and Cess[5] and Siegal and Howell[6] can be obtained by integrating this angular reflectance:

$$\rho_h(\lambda) = \int_0^{2\pi}\int_0^{\pi/2} \frac{\rho(\phi,\lambda)}{\pi}\cos\phi\sin\phi\,d\phi\,d\theta \tag{6}$$

or

$$\rho_h(\lambda) = \int_0^{2\pi}\int_0^{1} \frac{\rho(\mu,\lambda)}{\pi}\mu\,d\mu\,d\theta \tag{7}$$

This hemispherical reflectance and the corresponding monospectral hemispherical emittance are commonly used when radiant energy exchange is calculated. Judd[7] has calculated this hemispherical reflectance according to approximate formulas for internally and externally incident, perfectly diffuse monospectral light and compared his values to the values of reflectance at perpendicular incidence for the special case where k is equal to 0.0, i.e., dielectric material.

The total hemispherical reflectance is determined by integrating the monospectral hemispherical reflectance and the source function H_λ, per the following equation:

$$\rho_h = \int_0^\infty \rho_\lambda H_\lambda\,d\lambda \Big/ \int_0^\infty H\lambda\,d\lambda \tag{8}$$

This source function H_λ, represents the spectral distribution of the source irradiating the material of interest (n_λ, k_λ).

Results

Equation (7) was numerically integrated for a large variety of optical constants (n_λ, k_λ) for $N_0 = 1$. When these results were plotted with the results obtained from the Fresnel reflectance equation [i.e., Eqs. (1-5)] for $\phi = 60$ deg, an interesting pattern emerged. Figures 1-3 are typical examples. Included on these figures are dashed lines indicating lines of 5% and 10% error, as well as a solid line which indicates perfect agreement between $\rho_h(\lambda)$ and $\rho(60\text{ deg},\lambda)$. Using this type of information, Fig. 4 was deduced. Figure 4 presents values of n_λ and k_λ for which $\rho(60\text{ deg},\lambda)$ may be substituted for $\rho_h(\lambda)$ with expected errors of greater than 10%, between 5% and 10%, and less than 5%.

If the optical constants are known for a material, a fairly accurate estimate of the hemispherical reflectance value can be obtained merely by applying the Fresnel equations at the appropriate angle; that is, from Eq. (6),

$$\rho_h(\lambda) \doteq \rho(60\text{ deg},\lambda)$$

Received Oct. 27, 1978.

Index category: Radiation and Radiative Heat Transfer.

*Professor, Dept. of Mechanical Engineering, Thermal Radiative Transfer Group.